A Discrete Geometry Framework for Geometrical Product Specifications

M. Zhang[1], N. Anwer[1], L. Mathieu[1], H. B. Zhao[2],

[1] LURPA, Ecole Normale Superieure de Cachan, 61, avenue du President Wilson, Cachan, 94235, France

[2] PMA, Katholieke Universiteit Leuven, Celestijnenlaan 300b, Heverlee, 3001, Belgium

{min.zhang, anwer, mathieu}@lurpa.ens-cachan.fr

Haibin.Zhao@mech.kuleuven.be

Abstract

GeoSpelling as the basis of the Geometrical Product Specifications (GPS) standard [1] enables a comprehensive modeling framework and an unambiguous language to describe geometrical variations during the overall product life cycle. This is accomplished by providing a set of concepts and operations based on the fundamental concept of the "Skin Model". However, the definition of GeoSpelling has not been successfully completed. This paper presents a novel approach for a formal description of GeoSpelling concepts. In addition to mapping fundamental concepts and operations to discrete geometry objects, we investigate the use of Monte Carlo Simulation techniques for skin model simulation when considering geometrical specifications. The results of the skin model simulations and visualizations are shown and the performances of the described simulation methods are compared to each other.

Keywords:

Geometrical Product Specifications, GeoSpelling, Discrete geometry, Skin model, Multi-Gaussian distribution, Gibbs sampling

1 INTRODUCTION

The control of product geometrical variations during the whole development process is an important issue for cost reduction, quality improvement and company competitiveness in the global manufacturing era [2].

During the design phase, geometric functional requirements and tolerances are derived from the design intent. The modeling of product shapes and dimensions is now largely supported by geometric modeling tools. However, permissible geometrical variations cannot be intuitively assessed using existing modeling tools, and this results in the specification uncertainty.

In addition, the manufacturing and measurement stages are the main geometrical variations generators according to the two following axioms [3-4]:

- Axiom of manufacturing imprecision: all manufacturing processes are inherently imprecise and produce parts that vary.
- Axiom of measurement uncertainty: no measurement can be absolutely accurate and with every measurement there is some uncertainty about the measured value or measured attribute.

To reduce the total uncertainty, the product geometrical variations should be considered during the whole product life cycle (figure 1).

In order to evaluate product geometrical variations and ensure that the fabricated product can satisfy the functional requirements, designers should determine the limited values that constrain product geometrical variations. This process is now well known as specification.

In the context of Digital Mock-Ups (DMUs), the design process is supported by modeling, simulation and visualization tools such as CAD systems. The Digital Mock-Up, as a "digital" alternative to constructing physical parts, should be enriched by geometrical variation models to allow testing of design errors on assemblies and realistic visualization of the product. At the manufacturing level, multiple representations based on smooth surfaces and discrete representations (triangular meshes) are considered. Moreover, an ordered or unordered set of points resulting from manufactured part acquisition is processed for the purpose of product inspection.

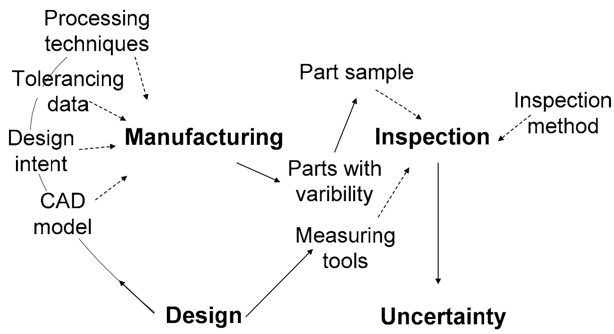

Figure 1: Geometrical variations during the product life cycle.

A comprehensive view of Geometrical Product Specifications should consider multiple geometric representations, and as well as suitable processing techniques and algorithms. The discrete geometry theory can offer a great support in this area, since discrete geometry is a mathematical research field related to geometrical objects whose nature or property is discrete. Therefore, it can provide the theory to handle both point and polyhedral mesh based descriptions.

The organization of this paper is as follows. After a comprehensive review of Geometrical Product Specifications and geometric tolerancing approaches (section 2) we show their limitations in considering multiple geometric representations and non-ideal entities. The principle of discrete geometry for GeoSpelling is described in section 3. Skin model simulation and visualization are highlighted in section 4. Afterwards, the skin model simulations which consider geometric tolerances and results comparison are developed in section 5. The conclusion is given in section 6.

2 RELATED WORK

Many efforts to build specification models for geometrical tolerancing have been attempted in recent years. The existing approaches can be mainly classified into standard-based and mathematical models for tolerancing .

The standard-based methods rely on technical drawings, and are based on the concepts of tolerance features, tolerance zones and datum. This geometrical tolerancing representation was adopted by ISO 1101-2004, ISO 5459-2000, and ASME Y14.5-2009, and it was the most popular way to describe tolerance requirements in the past years. However, this method cannot keep up with current tolerance requirements, since it is based on human interpretation and is not convenient to transfer the data what is now a digitally- based industry.

Mathematical models for tolerancing can be classified into several groups. The offset zone approach proposed by Requicha [5] obtains the tolerance zone by offsetting the ideal feature a certain distance and this method is suitable to geometrical models with simple shape representations. Jayaraman and Srinivasan introduced the Virtual Boundary Requirements (VBRs) method [6] to improve the offset zone method and to define the virtual boundary by mathematical foundations. The VBRs method considers assembly and material volume requirements. However, its shortcoming is that the results are not compatible with GPS standards and cannot describe all kinds of tolerances. Hoffman [7] and Turner [8] defined tolerancing models in different dimension spaces, and Fortini [9] introduced the vector tolerancing concept in parameter space, and then Wirtz [10] argued that vector tolerancing should be included in the ISO standards. The shortcoming of the vector tolerancing method is that it is not able to describe the tolerance features and the geometrical variation requirements. Bourdet and Clement [11] proposed the Small Displacement Torsor (SDT) theory, which can describe the tolerancing types by the small rigid displacement movement of geometric features. In contrast, this method is only appropriate for ideal features. Clement and Riviere [12] introduced the Technologically and Topologically Related Surfaces (TTRS) theory. According to TTRS, three-dimensional surfaces or features are classified according to their respective degree of invariance under the action of rigid motions. Basically, seven main features equivalent to kinematic lower pairs are identified: planar feature, cylindrical feature, revolution feature, spherical feature, prismatic feature, helicoïdal feature and complex feature. Each main feature is then described by a unique minimum geometrical reference element (MGRE) that allows positioning in Euclidean space. An MGRE is set as a combination of elementary geometrical objects: point, line and plane. TTRS Theory has been adopted by ISO TC213 and successfully implemented in the CATIA v5 CAD system to manage assembly constraints and tolerance annotations.

All of the methods described above cannot consider non-ideal features, and some of them even lead to ambiguous interpretations. The model of GeoSpelling [13] adopted by ISO-17450 allows a unified description of ideal and non-ideal features and permits a unique expression of mathematical parameterization of geometric features.

3 DISCRETE GEOMETRY FUNDAMENTALS OF GEOSPELLING

GeoSpelling proposed by Mathieu and Ballu [14] is used to describe both ideal and non-ideal geometric features [1]. Indeed, it allows the expression of product specifications from function to verification with a common language. This model is based on geometrical operations which are applied not only to ideal features defined by CAD systems, but also to the non-ideal features which can represent a real part. These operations include partition, extraction, filtration, association, collection and construction items.

Discrete geometry research focuses on basic discrete geometrical objects, such as points, segments, triangles and other convex discrete shapes, and it is quite efficient to implement digital discrete processing techniques.

Therefore, discrete geometry theories and techniques are suited to enhance the data processing capabilities of GeoSpelling. Based on the standard [4], a specification is defined as *a condition on a characteristic defined from geometric features which are created from a skin model by different operations*. The concepts of "characteristic," "feature," and "operation" are then mapped to their underlying discrete geometry mathematical concepts as summarized in table1.

	GeoSpelling	**Discrete Geometry**
Feature	non-ideal feature	point, segment, triangle, point set, polyline, mesh
	ideal feature	geometric shapes: plane, cylinder, sphere, …
Characteristic	distance	point to segment, point to triangle, segment to segment, segment to triangle
	angle	segment to segment, segment to plane, plane to plane
Operation	partition	segmentation
	extraction	sampling
	filtration	outlier removal, filtering
	association	approximation, interpolation
	collection	union-Boolean operation
	construction	intersection-Boolean operation

Table 1: Concepts mapping between GeoSpelling and discrete geometry.

3.1 Features

In GeoSpelling, features include non-ideal features and ideal features. In discrete geometry, non-ideal features are discrete shapes, such as points, segments, triangles, point sets, polylines, and polyhedral meshes. Ideal features are derived from the classification of 3D surfaces based on their invariance under the action of rigid motions. Ideal features can be obtained by association operations.

3.2 Characteristics

In GeoSpelling, characteristics include distances and angles. While in discrete geometry, distances are defined between discrete shapes: point-point, point-segment, point-triangle, segment-segment, segment-triangle and in a general case to Hausdorff distances. The angles are related to the three well-known cases: angles between segment-segment, segment-plane, and plane-plane.

3.3 Operations

Partition operation is used to identify bounded features [1]. In discrete geometry this kind of operation is called segmentation. The majority of point set segmentation methods can be classified into three categories: edge-detection method, region-growing method and hybrid method [15]. The main problem of the edge-based method is that when the points are near sharp edges they are quite unreliable. This problem means that the edge-based method has a relatively high sensitivity to occasional spurious points. The advantage of face-based techniques is that they work on a larger number of points to reduce the risk of sensitivity to occasional spurious points, and they can identify the points that belong to each surface, but the main disadvantage is time processing. The hybrid method has been developed by combining the edge-based and region-based methods together to overcome the limitations involved in the original methods.

Extraction operations are used to identify a finite number of points from a feature with specific rules [1]. In discrete geometry these rules are equivalent to sampling techniques. Zhang et al. [16] classified the extraction strategy into four categories: grid extraction, stratified extraction, special curve extraction and point extraction. Depending on the invariant class of the surface, users can determine the prior extraction strategy. Other extraction strategies were investigated in literature [17], such as Hammersley sequence sampling, the Halton-Zaremba sequence, Aligned systematic sampling, and Systematic random sampling.

Filtration operations are used to distinguish roughness, waviness, form, and so on, by separating the different wavelength components into predefined bandwidths [1]. There are already some options in today's GPS standards, such as polynomial fitting, 2RC filtering, Gaussian fitting, wavelet filtering, etc. [18]. In discrete geometry, signal processing filtering techniques and other techniques such as outlier removal, based on a certain criterion, are reported in [19].

Association operations are used to fit ideal feature(s) to non-ideal feature(s) according to specific rules [1]. In discrete geometry, association operations fit ideal feature(s) to discrete geometric feature(s) according to given criteria, such as the Moving Least Squares (MLS) method. MLS methods take the distance influence into account when calculating the association arithmetic [20].

Collection operations are used to consider some features together, which play a functional role, and construction is used to build ideal feature(s) from other ideal feature(s) [1]. In discrete geometry union-Boolean operations and intersection-Boolean operations [21] respectively have the same capability.

4 SKIN MODEL SIMULATION

The skin model is a non-ideal surface model. It is a virtual model imagined by designers when taking into account different kinds of geometric defects. The main originality of GeoSpelling is to build geometric models for tolerancing specification not from nominal models but from the skin model itself. It can also help designers to express specifications corresponding to manufacturing requirements. Few research studies have focused on the skin model simulation. Chiabert developed a shape identification method of the skin model using rigid body motion and Monte Carlo simulation [22]. Samper [23] proposed a finite element analysis method to simulate form defect expressions of skin models. However, there is no uniform way to express the skin model nowadays. Therefore, the skin model simulation method will be discussed here. Three different statistical methods are considered in this paper: 1D Gaussian distribution, multi-Gaussian distributions and Gibbs sampling. The details of each method are explained below.

4.1 1D-Gaussian method

In probability theory, the Gaussian distribution is a continuous probability distribution that is often used as a first approximation to describe real-valued random variables that tend to cluster around a single mean value. The graph of the associated probability density function is "Bell"-shaped as showed in figure 2.

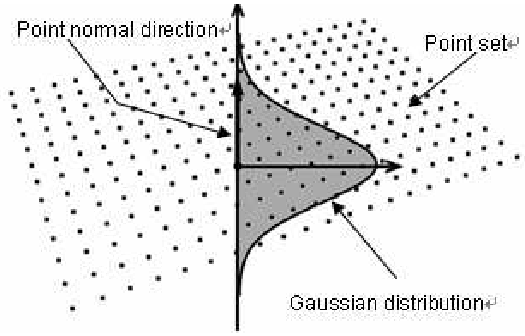

Figure 2: The principle of 1D-Gaussian method.

The principle of the 1D-Gaussian method can be described in figure 2. The "bell" shape reflects the scope of the 1D-Gaussian distribution acting on one point. It is a random value and it can be calculated by the probability density function of the 1D-Gaussian (Formula 1). In this formula, the mean value is the input points' coordinates, and the variance determines the width of the Gaussian distribution. This method uses the Gaussian variable as the deviation value in the direction of vertex normal (the vertex normal estimation method is explained in section 3.3), then it applies this calculation to each point, the distribution parameters yield formula 2, and then the result is illustrated in figure 3 with different views of the skin model of a plane.

$$X \approx N(\mu,\sigma^2) : f(x) = \frac{1}{\sigma\sqrt{2\pi}} e^{-\frac{(x-\mu)^2}{2\sigma^2}} \qquad (1)$$

$$u = \frac{X-\mu}{\sigma} \approx N(0,1) \qquad (2)$$

Where μ is the mean value, σ^2 is the variance, and x is the Gaussian variable.

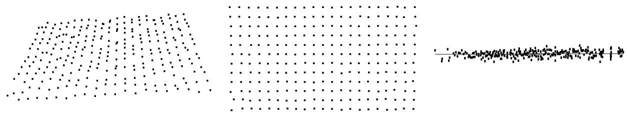

(a) skin model (b) front view (c) left view

Figure 3: 1D-Gaussian skin model.

4.2 Multi-Gaussian method

A multivariate Gaussian distribution is used to generate random vectors. The trivariate Gaussian distribution is considered in this work. A spatial random vector is defined as $X = (X_1, X_2, X_3)^T$. The probability density function of multivariate Gaussian distribution can be expressed as formula 3.

$$X \approx N(\mu,\Sigma) : f(x) = \frac{1}{(2\pi)^{3/2}|\Sigma|^{1/2}} \exp(-\frac{1}{2}(x-\mu)^T \Sigma^{-1}(x-\mu)) \qquad (3)$$

Where Σ is the covariance matrix, $|\Sigma|$ is the determinant value, and μ is the mean vector.

The principle of this method is described in figure 4. The ellipsoid reflects the scope of 3D-Gaussian distribution acting on one point. It is a random vector and can be calculated by the probability density function of the 3D-Gaussian (formula 3). In this formula, the mean value is the point's coordinates, and the relationships among each axis are constrained by the covariance matrix. Figure 5 displays different views of the skin model of a plane when applying this calculation to each point.

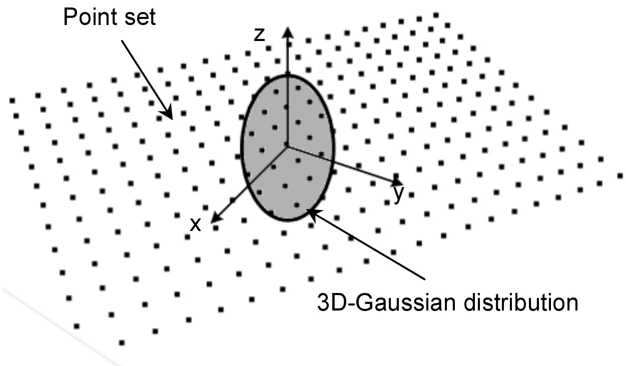

Figure 4: The principle of 3D-Gaussian method.

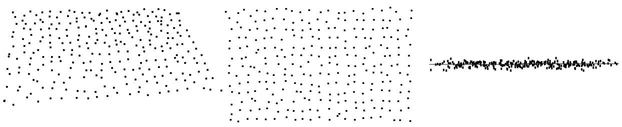

(a) skin model (b) front view (c) left view

Figure 5: 3D-Gaussian skin model.

4.3 Gibbs Method

The Gibbs sampling algorithm is used to generate a sequence of samples from the joint probability distribution of two or more random variables. It is an iterative method based on Markov chain Monte Carlo (MCMC) algorithms. It aims to design a Markov chain whose stationary distribution is the target distribution. It requires an initial value of the parameters, and at each iteration, each parameter of interest is sampled a given value from the other parameters and data. Once all the parameters of interest are sampled, the nuisance parameters are sampled given the parameters of interest and the observed data [24-25]. This characteristic of the Gibbs method can make the random distribution of point set of skin models approximate a Gaussian distribution.

In order to determine the number of iterative runs, the probability distribution of the normality assumptions of Gibbs should be considered. The normal distributions are simulated using Minitab software for different iterative runs (figure 6). The results show a good convergence at 10000 iterations.

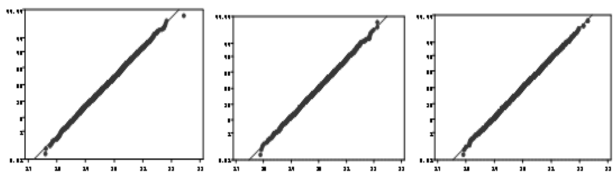

(a) N=10 (b) N=100 (c) N=10000

Figure 6: Normality assumption of Gibbs method.

Suppose $X = (X_1, \ldots, X_d)$ is the random value in R^d, and $X_{-j} = (X_1, \ldots, X_{j-1}, X_{j+1}, \ldots, X_d)$ is the random value of $d-1$ dimension. Note that the conditional density function of $X_j \mid X_{-j}$ is $f(X_j \mid X_{-j})$. Therefore, the Gibbs sampler select candidate points from this dimension conditional distribution. The related process is that, at beginning, the time is equal to zero ($t = 0$) and it has an initial value $X(0)$. When t is increasing ($t = 1, 2, \ldots, T$), then $X(t)$ follows a certain function to generate new point to replace old one and iterative calculation is performed until it converges to the target value. The corresponding pseudo-code is described as follow.

1. Let $x_1 = X_1(t - 1)$
2. Let j is a variable between $[1, d]$. For $j = 1, 2, \ldots, d$, using $f(X_j \mid x_{-j})$ to get candidate point $X_j^*(t)$, and then update $X_j^*(t)$.
3. Let $X(t) = (X_1^*(t), \ldots, X_d^*(t))$ and then increase t.

This iterative process generates random variables, which follow the bivariate normal distribution, can simulate the skin model. The result is showed in figure 7.

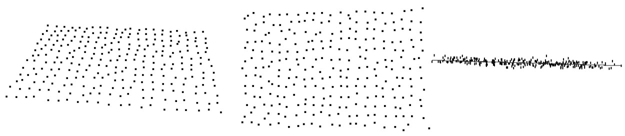

(a) skin model (b) front view (c) left view

Figure 7: Gibbs Sampling Skin model.

4.4 Skin model visualization

Tolerance values are much smaller than features' sizes, so it is difficult to visualize the skin model with multi-scale geometry. This section proposes to use RGB color scale mapping technique to visualize the geometrical deviations on the vertex normal direction. The skin model can be reflected by a continuous color strip.

Vertex normal estimation

A normal vector is a local geometric property of a 3D surface, which is specific to a given point or a planar facet. Many attempts have already been made for reliable estimation of normal vectors from discrete point data [15].

Given a polyhedral mesh surface, the normal vector at a vertex can be estimated as the weighted average of the normal vectors of the adjacent triangle facets around it. Considering an arbitrary vertex p in a discrete mesh surface Σ, assuming its neighbor contains N triangles, then the normal vector at p could be estimated using formula 4.

$$\boldsymbol{n}(p) = \frac{\sum_{i=1}^{N} \omega_i \cdot \boldsymbol{n}_i}{\left\| \sum_{i=1}^{N} \omega_i \cdot \boldsymbol{n}_i \right\|} \quad (4)$$

Where, $\boldsymbol{n}_i$ $(i = 1, \ldots N)$ indicate the unit normal vector of the i th triangle facet. ω_i ($i = 1, \ldots N$) are the weight coefficients corresponding to the normal vectors of facets f_i.

The method used here for the weight coefficients computation considers the influence of the area of each adjacent triangle facet and the distance between the given vertex and the barycenter of each adjacent facet. Parameter ω_i can be calculated by formula 5.

$$\omega_i = \frac{A_i / d_i^2}{\sum_{i=1}^{N} A_i / d_i^2} \tag{5}$$

Where, A_i ($i = 1,\ldots N$) represents the area of the i th triangle facet. d_i ($i = 1,\ldots N$) are the distances between the vertex p and the barycenter of the i th triangle facet. Parameter N is the number of all the triangle facets adjacent to the given vertex.

The notations mentioned in the above formula are described in figure 8. Figure 9 shows examples of vertex normal estimation considering planar and cylindrical shapes.

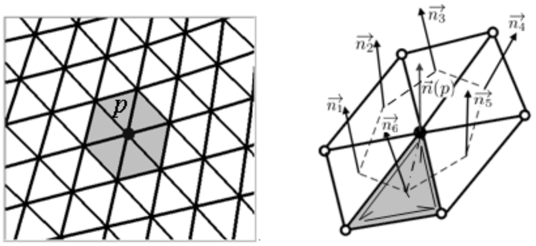

(a) mesh structure (b) vertex normal

Figure 8: Vertex normal estimation.

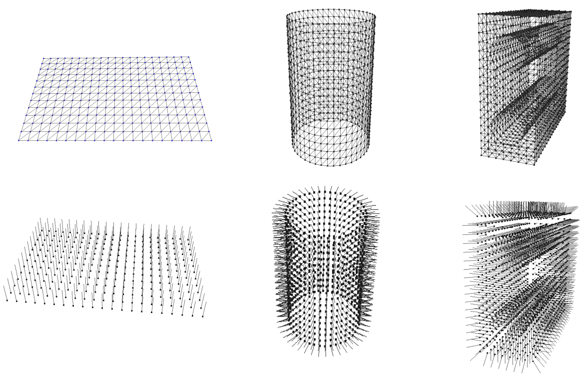

Figure 9: Example of vertex normal estimation on discrete shapes.

RGB mapping technique

The geometrical deviations between the simulated skin model and the initial point set are computed by projecting the deviation vectors on the vertices normal. A continuous RGB color scale is then used to visualize the skin model (figure 10).

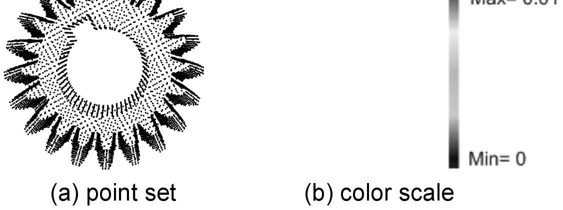

(a) point set (b) color scale

Figure 10: Skin model with color scale.

5 CONSTRAINT-BASED SKIN MODEL

After creating the random point set to simulate the unconstrained skin model, geometrical and dimensional tolerances should be considered to satisfy the specification requirements. The following section mainly discusses the form, orientation and position tolerance considerations to enhance the skin model simulation.

Form specification

To estimate form specification, the first step is to determine the tolerance zone direction using the Principal Component Analysis (PCA) method. Then all of the point set should belong to the tolerance zone. The principle of this method can be described by figure11, where $\boldsymbol{n}$ is the vector of principle direction of the point set, M_1 and M_2 are two arbitrary points, and d is the distance between these two points in the direction of the vector $\boldsymbol{n}$.

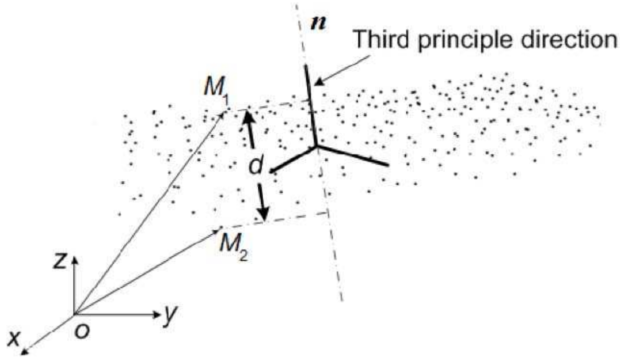

Figure 11: Principle of flatness specification.

PCA is a statistical method for principal component analysis by covariance analysis.

Consider a discrete shape P_N represented by an arbitrary set of points $P_i = [x_i, y_i, z_i]^T$. The PCA method computes the principal axes of the discrete shape using the following three steps.

1. The origin of the principal coordinates system is determined as the centroid of P_N which is calculated by formula 6.

$$o_{pca} = \frac{1}{N}\sum_{i=1}^{N} p_i \quad (p_i \in P_N) \tag{6}$$

2. The covariance matrix is defined by formula 7.

$$M_{\text{cov}} = \sum_{i=1}^{N} (p_i - o_{pca})(p_i - o_{pca})^T \quad (p_i \in P_N) \tag{7}$$

3. Eigenvalues and eigenvectors are estimated. The first principal axis is the eigenvector corresponding to the largest eigenvalue. The two other principal axes are obtained from the remaining eigenvectors.

The tolerance zone direction is determined using the PCA method, and the point set should satisfy the tolerance zone constraint (formula 8).

$$\left| Max(\boldsymbol{m}_i \cdot \boldsymbol{n}) - Min(\boldsymbol{m}_i \cdot \boldsymbol{n}) \right| \le t_{flatness} \tag{8}$$

Where $\boldsymbol{m}_i$ is the vector of i th point, and $\boldsymbol{n}$ is the vector of tolerance direction, $t_{flatness}$ is the flatness tolerance value.

Orientation and position specification

Besides form constraints, the orientation and position constraints must also be considered. For these two constraints, the tolerance direction is the same as the normal direction of the datum plane and all the points should be within the tolerance zone.

The parallelism specification (figure 12) satisfies the constraints in formula 9.

$$d = \left| Max(\boldsymbol{m}_i \cdot \boldsymbol{n}) - Min(\boldsymbol{m}_i \cdot \boldsymbol{n}) \right| \leq t_{parallelism} \qquad (9)$$

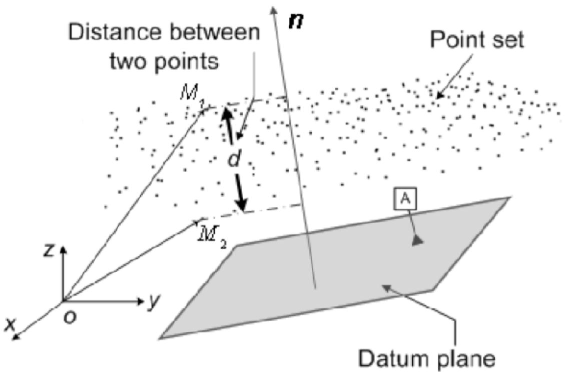

Figure 12: Principle of parallelism specification.

Where $\boldsymbol{n}$ is the normal direction of the datum plane, M_i is an arbitrary point, and d is the distance between two points in the direction of vector $\boldsymbol{n}$.

For position specification (figure 13), the related constraint is described by formula 10.

$$d = Dist(m_i, P_A) \in [a - \frac{t_{position}}{2}, a + \frac{t_{position}}{2}] \qquad (10)$$

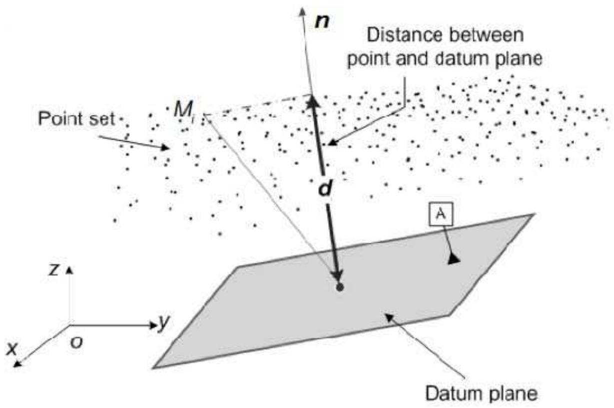

Figure 13: Principle of position specification.

Where $\boldsymbol{n}$ is the normal direction of the datum plane, M_i is an arbitrary point, and d is the distance between the point to datum plane P_A in the direction of vector $\boldsymbol{n}$, and a is the nominal distance value of position tolerance.

Comparisons

The skin model is created using the three different simulation methods proposed in this paper. A point cloud of a plane composed by 273 points is the reference test, and the specification constraints are flatness, parallelism and position tolerances which are equal to 0.01 mm, 0.02 mm and 0.05 mm respectively. The 50 skin models are generated and the main statistical characteristics are computed for comparison. In the Gibbs sampling method, the iterative time is equal to 10000.

The comparison items include the average deviation value, the limit value, and the processing time. The distribution of the deviation values is computed using Minitab statistical software. The result is shown in figure 14. Corresponding standard deviations are summarized in table 2. From this table, it can be deduced that the Gibbs method offers the closest simulation result to the target value, but it is much more time consuming.

Items	1D-Gaussian	3D-Gaussian	Gibbs
Average Value	0.008666	0.008705	0.008883
Standard deviation	0.000567	0.001287	0.000521
Maximum value	0.009869	0.009831	0.009778
Minimum value	0.006943	0.000510	0.007488
Time	<0.001 s	<0.001 s	0.297s

Table 2: Results of comparison of the three methods.

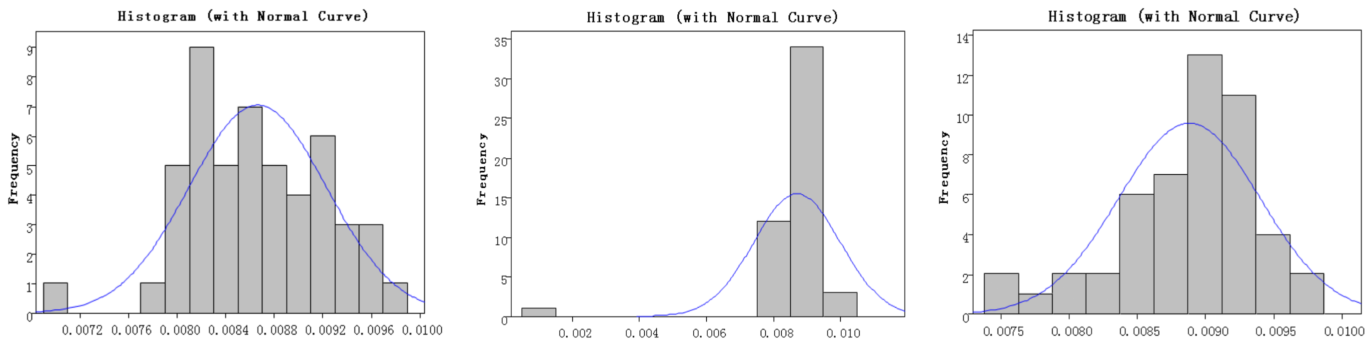

(a) 1D-Gaussian method (b) 3D-Gaussian method (c) Gibbs method

Figure 14: Statistical distribution results.

6 SUMMARY AND CONCLUDING REMARKS

In this paper, we saw that discrete geometry for GeoSpelling provides a new mathematical framework for Geometrical Product Specifications. Starting from the fundamental concepts of the skin model and non-ideal features, skin model simulation and visualization using 1D Gaussian, 3D-Gaussian and Gibbs method is developed and compared.

With new foundations for Geometrical Product Specifications, this paper concludes that discrete geometry and statistical shape techniques are promising approaches towards skin model consideration during the product life cycle.

7 ACKNOWLEDGMENTS

The first author extends the sincere thanks to the China Scholarship Council (CSC) for their financial support for this work.

8 REFERENCES

[1] ISO 17450: 2005. Geometrical Product Specifications (GPS) – General concepts – Part 1: Model for geometrical specification and verification .

[2] Anwer, N., Cid, G., Mathieu, L., 2003, XML based tolerance management for integrated design, International CIRP Design Seminar, Grenoble, (12):12-14.

[3] Srinivasan, V., 2007, Computational metrology for the design and manufacture of product geometry : A classification and synthesis, Journal of computing and information science in engineering, vol. 7(1), pp. 3-9.

[4] Ballu, A., Plantec, J.-Y., Mathieu, L., 2008, Geometrical reliability of overconstrained mechanisms with gaps, Annals of the CIRP, (57):45-49.

[5] Requicha, A.A.G., 1983, Solid Modeling: Current Status and Research Directions, IEEE Computer Graphics & Applications. (10): 25-37.

[6] Jayaraman, R., Srinivasan V., 1989, Geometric Tolerancing: I. Virtual Boundary Requirements, IBM Journal of Research and Development, (33): 90-104.

[7] Hoffman, P., 1982, Analysis Tolerances and Process Inaccuracies in Discrete Part Manufacturing. Computer Aided Design, 14(2): 178-186.

[8] Turner, J. U., 1990, The M-space Theory of Tolerances. Proceedings of the ASME Advances in Design Automation conference, 217-225.

[9] Fortini, E., 1967, Dimensioning for Interchangeable Manufacture. Industrial Press Inc.

[10] Wirtz, A., Gachter, Chr., Wipf, D., 1993, From Unambiguously Defined Geometry to the Perfect Quality Control Loop. CIRP Annals-Manufacturing Technology, 42(1): 615-618.

[11] Bourdet, P., Clement, A., 1988, A study of optimal-criteria identification based on the small displacement screw model, Annals of the CIRP, (37): 503-506.

[12] Clement, A., Riviere, A., Serre, P., 1995, A declarative information model for functional requirements, Proceedings of 4th CIRP Seminars on Computer Aided Tolerancing, ISBN: 0412727404, 1-15.

[13] Ballu, A., Mathieu, L., 1995, Univocal expression of functional and geometrical tolerances for design, manufacturing and inspection. Computer Aided Tolerancing 4th CIRP Seminar, ISBN: 0412727404, 31-46.

[14] Mathieu, L., Ballu, A., 2003, GEOSPELLING: a common language for Specification and Verification to express Method Uncertainty. Proc. Of 8th CIRP Seminar on Computer Aided Tolerancing, The University of Charlotte, North Carolina, USA; April, 28-29.

[15] Zhao, H.B., 2010, Multisensor integration and discrete geometry processing for coordinate metrology. PhD thesis, ENS Cachan, Jan.

[16] Zhang, L.N., Zheng, Y.H., Zheng, P., 2007, Model of extraction operation and the Research of its Application Specification Based on GPS, Journal of Mechanical Strength, 29(4): 632-636.

[17] Kim, W.S., Raman, S., 2000, On the selection of flatness measurement points in coordinate measuring machine inspection, International Journal of Machine Tools & Manufacture, (40): 427-443.

[18] Jiang, X.Q., 2007, Theory and Applications of New-Generation Geometrical Product Specificaitons, Higher Education Press, ISBN：9787040224894, 148-164.

[19] Gross, K., Pfister, H., 2007, Point-based Graphics. Morgan Kaufmann.

[20] Lancaster, P., Salkauskas, K., 1981, Surfaces Generated by Moving Least Squares Methods, Mathematics of Computation. 37(1): 141-158.

[21] Mark, B., Kreveld, M.V., Overmars, M., etc., Computer Geometry: Algorithms and Applications, ISBN: 9783540779735, 39-40.

[22] Chiabert, P., Maddis, M. D., 2005, Statistical modeling of geometrical invariant sampled sets, CIRP International Seminar on Computer Aided Tolerancing. Tempe, Arizona, USA, 10-12.

[23] Samper, S., Formosa, F., 2007, Form Defects Tolerancing by Natural Modes Analysis. Journal of Computing and Information Science, March, (7): 44-51.

[24] Eric, C., 1997, A Brief Overview of Gibbs Sampling. Washington University Institute for Biomedical Computing Statistics Study Group. May.

[25] Xavier, E., 2007, Using the Gibbs sampler for conditional simulation of Gaussian-based random fields, Computers& Geosciences, (33): 522-537.